CROSS-COMPATIBILITY OF AERIAL AND TERRESTRIAL LIDAR FOR QUANTIFYING FOREST STRUCTURE

by

Franklin Wagner

A Thesis

Submitted to the Faculty of Purdue University

In Partial Fulfillment of the Requirements for the degree of

Master of Science

Department of Forestry & Natural Resources

West Lafayette, Indiana

August 2019

THE PURDUE UNIVERSITY GRADUATE SCHOOL
STATEMENT OF COMMITTEE APPROVAL

Dr. Brady Hardiman, Co-Chair

Department of Forestry and Natural Resources

Dr. Songlin Fei, Co-Chair

Department of Forestry and Natural Resources

Dr. Ayman Habib

Lyles School of Civil Engineering

Approved by:

Dr. Robert G. Wagner

Head of the Graduate Program

This document is dedicated to all the educators, colleagues, friends, and family who have made my academic endeavors up to this point a reality, and to those who aspire to pursue humanity's further conservation of the natural world.

TABLE OF CONTENTS

LIST OF TABLES

LIST OF FIGURES

ABSTRACT

Author: Wagner, Franklin, W. MS
Institution: Purdue University
Degree Received: August 2019
Title: Cross-Compatibility of Aerial and Terrestrial Lidar for Quantifying Forest Structure
Committee Chair: Brady Hardiman, Songlin Fei

Forest canopies are a critical component of forest ecosystems as they influence many important functions. Specifically, the structure of forest canopies is a driver of the magnitude and rate of these functions. Therefore, being able to accurately measure canopy structure is crucial to ensure ecological models and forest management plans are as robust and efficient as possible. However, canopies are complex and dynamic entities and thus their structure can be challenging to accurately measure. Here we study the feasibility of using lidar to measure forest canopy structure across large spatial extents by investigating the compatibility of aerial and terrestrial lidar systems. Building on known structure-function relationships measured with terrestrial lidar, we establish grounds for scaling these relationships to the aerial scale. This would enable accurate measures of canopy structural complexity to be acquired at landscape and regional scales without the time and labor requirements of terrestrial data collection. Our results illustrate the potential for measures of canopy height, vegetation area, horizontal cover, and canopy roughness to be upscaled. Furthermore, we highlight the benefit of utilizing multivariate measures of canopy structure, and the capacity of lidar to identify forest structural types. Moving forward, lidar is a tool to be utilized in tandem with other technologies to best understand the spatial and temporal dynamics of forests and the influence of physical ecosystem structure.

CHAPTER 1. TERRESTRIAL VS AERIAL LASER SCANNING

1.1 Introduction

1.1.1 Canopy Structure as a Forest Attribute

Understanding forest ecosystem structure (i.e., the physical arrangement and distribution of vegetation) is of critical importance as it directly influences a wide range of ecosystem functions. Canopy structure, the 3-D arrangement of vegetation within the canopy volume, and in turn canopy structural complexity, has been shown to influence ecosystem functions such as primary production (Hardiman et al. 2011), radiation balance and gas exchange (Parker et al. 2004a, Atkins et al. 2018a), habitat provisioning (Bergen et al. 2009), and nutrient cycling (Hardiman et al. 2013). In fact, canopy structure can be a more effective predictor of some ecosystem functions, such as light interception, than more commonly measured variables such as leaf area index (LAI) (Atkins et al. 2018). More structurally complex canopies allow for more effective absorption of incoming solar radiation, as plants use diffuse light more efficiently than direct light (Li et al. 2015) and a more complexly arranged canopy facilitates the transmission and interception of diffuse light throughout the canopy. Structure-function relationships such as this relate to the intrinsically dynamic nature of canopy structure, the mechanics of which involve complex interactions between abiotic factors, disturbance regime, species composition, and stand structure (Fotis et al. 2018).

The complex nature of forest canopies makes them challenging to accurately measure, however, doing so has the potential to dramatically improve characterization and modeling of structure-function relationships. Being able to characterize forest attributes at fine scales is necessary for forest management that replicates natural conditions as closely as possible (Zimble et al. 2003, Fahey et al. 2018). Characterizing horizontal forest structure has been established for decades (through techniques such as hemispherical photography and traditional forest inventories),

but accurately quantifying the complexity of vertical structure has proven to be more elusive. Most remotely sensed optical imagery is limited in the inferences that can be made when used in settings with multi-layered and dense forest vegetation, and commonly is reliant on electromagnetic energy radiated from the earth and thus limited in the data resolution that is achievable.

1.1.2 Lidar as a Tool for Measuring Canopy Structure

Lidar (light detection and ranging) has the capability to measure horizontal *and* vertical canopy structure, and has been widely demonstrated to be an effective method for characterizing functionally-relevant forest structures (e.g. Lefsky et al. 2002a, Lim et al. 2003, Nguyen et al. 2016, Disney et al. 2018, Larue et al. 2018). Terrestrial laser scanning (TLS) can measure metrics of internal canopy structure with important links to ecosystem functions at high resolution (Hopkinson et al. 2004, Hardiman et al. 2011, Atkins et al. 2018a, Almeida et al. 2019). However, it is logistically challenging to deploy across large spatial extents and can be both time and labor intensive. Conversely, aerial laser scanning (ALS) sacrifices high data resolution for the ability to measure structure over wide spatial extents. Therefore, integrating aerial and terrestrial lidar would enable accurately measuring forest structure to understand ecological patterns and processes from local to large spatial scales. This advancement would prove pivotal for ecosystem modeling, forest management decision making, and the design of conservation strategies, as well as for facilitating integration with other remote sensing data products and large-scale climate models.

There have been a few studies that explicitly investigated the relationship between aerial and terrestrial structural measures (Hilker et al. 2010, Listopad et al. 2011, Hilker et al. 2012, Hopkinson et al. 2013). However, these studies have been limited to the extent of a single study site primarily dominated by a single species, which tend to have simpler structure compared to forest landscapes throughout most of the eastern United States. Additionally, these studies have

not explored relationships between aerial and terrestrial structural complexity metrics. This suggests that these conclusions may be dependent on the structural attributes of a specific site or community type, limiting the generalizability of conclusions.

1.1.3 Study Objective

The objective of our study was to investigate the relationship between aerial and terrestrial lidar across a range of forest ecosystem types to establish the feasibility of upscaling functionally relevant terrestrial metrics to the scale of aerial data collection. This would enable detailed aerial measurements in areas where terrestrial data is not available. We aimed to evaluate the strength of correlation between a suite of aerially derived structural metrics and terrestrially derived metrics. We further explored the agreement between aerial and terrestrial lidar using multivariate measures of structure.

1.2 Methods

1.2.1 Study Sites

This study was carried out at plots (n=88) from seven National Ecological Observatory Network (NEON) sites across the eastern United States. These sites (Table 1.1) were chosen for their structural diversity and the availability of terrestrial data collected. The aerial data were acquired by NEON and downloaded via NEON's online data depot. Each plot from which data were acquired is 1600 m^2 (40 m x 40 m).

Table 1.1. NEON study sites.

Site	State	NEON Domain	Dominant Forest Type	Plots
Harvard Forest (HARV)	Massachusetts	D01: Northeast	Mixed Temperate	19
Smithsonian Conservation Biology Institute (SCBI)	Virginia	D02: Mid-Atlantic	Mixed Temperate	6
Smithsonian Environmental Research Center (SERC)	Maryland	D02: Mid-Atlantic	Temperate Deciduous	13
Ordway-Swisher Biological Station (OSBS)	Florida	D03: Southeast	Pine Savannah	20
University of Notre Dame Environmental Research Center East (UNDE)	Michigan	D05: Great Lakes	Mixed Temperate	8
Great Smoky Mountain National Park (GRSM)	Tennessee	D07: Appalachians & Cumberland Plateau	Temperate Rainforest	10
Talladega National Forest (TALL)	Alabama	D08: Ozarks Complex	Pine Savannah	12

1.2.2 Lidar Systems and Data Collection

The aerial system (Optech ALTM Gemini; Table 1.2) exists as a whiskbroom scanning sensor deployed on an aerial observation platform (AOP) and flown over the study sites producing a three-dimensional point cloud. The terrestrial system (Riegl LD90-3100VHS-FLP; Table 1.2) exists as a portable canopy lidar (PCL), of which the design, operation, and validation can be found in Parker et al. (2004b). In short, the user walks along a pre-laid transect collecting data linearly, where the data product is a 2-D plane with one axis being the length of transect walked and the other being the height above the sensor with corresponding lidar return heights. Three parallel transects were laid per plot (see Atkins et al. 2018a for detailed field methods).

Table 1.2. Lidar system specifications.

System Specifications	Optech ALTM Gemini (ALS)	Riegl LD90-3100VHS-FLP (TLS)
Returns per Pulse	Four	Five
Wavelength	1064 nm	900 nm
Measurement Range	150 - 4000 m AGL	60 m ($\rho \geq 0.1$) - 200 m ($\rho \geq 0.8$)
Range Accuracy (typical)	± 5 - 30 cm	± 2.5 cm
Bean Divergence Angle	0.25 mrad x 0.8 mrad	3 mrad x 5 mrad
Measurement Rate (per second)	0 - 70 (programmable)	2,000
Average Point Density	1 - 4 points per m^2 < 1 point per m^3	2,000 - 10,000 points per linear meter
Laser Product Classification	Class IV (US FDA 21 CFR)	IEC 60825-1:2007 (Eye-safe)

1.2.3 Structural Metric Suites

A suite of aerial (Table 1.3) and terrestrial (Table 1.4) metrics were generated due to the different data attributes and workflows associated with the aerial and terrestrial systems. These metrics fall into four categories that characterize different aspects of canopy structure: (1) *canopy height,* (2) *leaf area and density,* (3) *canopy cover and openness,* and (4) *canopy heterogeneity* (Atkins et al. 2018a). Metrics in the canopy height category include mean canopy height, maximum canopy height, and mean outer canopy height. Vegetation area index (VAI) is the metric contained within the leaf area and density category. Canopy cover and openness includes measures of canopy gap and cover fraction. The final category, canopy heterogeneity, includes a total of 16 metrics that characterize canopy structural complexity.

Table 1.3. Aerial lidar structural metric suite. Included is the structural category of each metric along with a short description. All metrics derived using the R programming language.

Metric	Category	Description	Unit
Mean Canopy Height	Height	Mean canopy height of lidar point cloud	m
Mean Outer Canopy Height	Height	Mean of maximum canopy height from lidar canopy height model (CHM)	m
Maximum Canopy Height	Height	Maximum canopy height in CHM	m
Vegetation Area Index (VAI)	Vegetation	Summation of leaf area density in 1 m layers of lidar point cloud	N/A
Deep Gaps	Cover & Openness	Number of pixels in CHM with zero canopy returns	count
Deep Gap Fraction	Cover & Openness	Number of deep gaps divided by total number of CHM pixels	0-1
Cover Fraction	Cover & Openness	Number of CHM pixels with height above ground height divided by total number of CHM pixels	0-1
Gap Fraction Profile	Cover & Openness	Mean gap fraction of 1 m layers in lidar point cloud	0-1
Rumple	Heterogeneity	Ratio of outer canopy surface area to ground surface area	ratio
Top Rugosity	Heterogeneity	Standard deviation of CHM heights	m
Height SD (lidR)	Heterogeneity	Standard deviation of lidar point cloud return heights	m
Height SD (rLiDAR)	Heterogeneity	Standard deviation of lidar point cloud return heights	m
SD of Vertical SD of Height	Heterogeneity	Standard deviation of rasterized standard deviation of lidar point cloud return heights	m
Entropy	Heterogeneity	Measure of evenness of lidar returns in 1 m layers; values closer to 1 represent a more even distribution of returns across the layers	0-1
Vertical Complexity Index	Heterogeneity	A fixed normalization of entropy	0-1

Table 1.4. Terrestrial lidar structural metric suite. Included is the structural category of each metric along with a short description. All metrics derived using the R programming language.

Metric	Category	Description	Unit
Mean Leaf Height	Height	Transect mean of columnar leaf height	m
Mean Outer Canopy Height	Height	Transect mean of columnar maximum canopy height	m
Maximum Canopy Height	Height	Maximum columnar canopy height along transect	m
Mean of Squared Leaf Height Mode (Mode.2)	Height	Transect mean of squared columnar leaf height mode	m
Mode.el	Height	Transect mode height of maximum VAI return in each column along transect	m
Mean Height of Maximum VAI (Max.el)	Height	Transect mean height of maximum VAI return in each column along transect	m
Mean VAI	Vegetation	Mean of columnar summed vegetation area index (VAI)	N/A
Mean Peak VAI	Vegetation	Mean of VAI_{max} (maximum x,z value of VAI)	N/A
Deep Gaps	Cover & Openness	Number of 1 m columns with no LiDAR returns	count
Deep Gap Fraction	Cover & Openness	Total number of deep gaps divided by transect length	0-1
Sky Fraction	Cover & Openness	Transect mean of columnar ratio of sky hits to total vegetation returns	0-1
Cover Fraction	Cover & Openness	Transect mean of columnar ratio of canopy returns to total vegetation returns	0-1
Canopy Rugosity	Heterogeneity	Transect variability of columnar leaf density variability	m
Top Rugosity	Heterogeneity	Transect variability of columnar maximum canopy height	m
Rumple	Heterogeneity	Ratio of outer canopy surface area to underneath ground surface area	ratio
Mean of Vertical SD	Heterogeneity	Transect mean of columnar mean leaf height variability	m
SD of Vertical SD	Heterogeneity	Standard deviation of columnar mean leaf height variability	m
Effective Number of Layers (ENL)	Heterogeneity	Occupation of 1 m layers by vegetation relative to total space occupation	count
Root Mean Square Height	Heterogeneity	Root mean square of columnar mean leaf height	m
Mean Height Variability	Heterogeneity	Transect variability of columnar mean leaf height	m
SD of Mean Height (Height.2)	Heterogeneity	Standard deviation of columnar mean leaf height	m

1.2.4 Data Processing and Metric Preparation

Processing of the collected lidar data was performed using the R programming language (The R Group), specifically the *forestR, lidR* and *rLiDAR* packages (Atkins et al. 2018, Roussel et al. 2018, Silva et al. 2017). The processing of the terrestrial data is linked to the means of data collection. As the PCL produces a 2-D plane, this plane is partitioned into one-meter wide columns along the transect (i.e. a transect of 40 meters would be divided in to 40 one-meter wide columns). The plane is further divided in to one-meter tall rows, resulting in the data plane being completely partitioned in to 1 m^2 'bins' in which each bin is weighted relative to the total number of lidar returns that fell in its respective area. Metrics were collected from three parallel transects and averaged per plot to gain a single mean value. Metrics are calculated by deriving various columnar-transect combinations and relationships. For example, mean outer canopy height derived from the PCL system corresponds to the mean of the maximum returned height in each one-meter column along a transect. All PCL metrics were derived using the f*orestR* package (Atkins et al. 2018b).

NEON level-1 aerial point clouds are not standardized to ground height and thus the return heights must be standardized using a digital terrain model (DTM) in order to correct for topography. To account for edge effect, a buffer zone around each plot was used in deriving the DTM. Plot-level point clouds were clipped from the site-level point clouds using plot centroid coordinates acquired via the NEON data depot. Some aerial metrics are derived directly from the ground-standardized plot point cloud while others are derived from a canopy height model (CHM) generated at a resolution of 1 m^2, with each 1 m^2 pixel being assigned a value corresponding to the highest lidar return in that equivalent area from the point cloud. Taking mean outer canopy height as an example again, this was derived by calculating the mean value of all CHM pixels within the full 1600 m^2 plot extent. All aerial metrics were derived with the *lidR* and *rLiDAR* packages (Roussel et al. 2018, Silva et al. 2017).

1.2.5 Evaluating Aerial and Terrestrial Structural Metrics

Due to the 2-D nature of the terrestrial data and 3-D nature of the aerial data, we evaluated the impacts of sampling area on aerial metrics to better understand the correlation between terrestrial and aerial measurements. A collection of 'slice widths' ranging from 0.5 m (i.e. a 0.5 m x 40 m slice) up to 40 m (full plot extent) was used to evaluate the sensitivity of aerial metrics to sampling area. As the PCL system captures a 'slice' through the canopy, we aimed to establish if a 'slice' of area from the aerial data produced similar results to metrics derived using a full plot. A total of 14 slice widths were evaluated with 10 randomized iterations of each width. The 10 randomizations were performed by using the plot edge coordinates as the range from which the coordinates of each slice were randomized using a random number generator in R. In this sense, the slices can be thought of as a slider bar bouncing back and forth between the plot edges, with random coordinates being chosen as the area from which metrics were calculated.

To investigate correlation strengths between aerial and terrestrial metrics, we calculated the Pearson's correlation coefficient (r) of each pairwise combination of aerial and terrestrial metrics within each category. To facilitate interpretation, we used common cut-off values by defining $|r| \geq 0.7$ as a strong correlation and $|r| \geq 0.5$ as a moderate correlation.

In addition to the pairwise correlation analysis, which provides relatively simple two-dimensional similarity between metrics, we performed two multivariate ordination analyses. First, we performed a non-metric multidimensional scaling (NMDS) operation to evaluate clustering agreement between the aerial and terrestrial metric suites. Similar partitioning of the study plots by site would be reflective of agreement between the two systems. Data was standardized to correct for differences in magnitude and the ordinations were performed using Euclidean distances and twenty maximum iterations. A principal component analysis (PCA) was also performed to identify the most influential structural metrics across the various sites. Like the NMDS, similar axis

loadings between the aerial and terrestrial PCA would indicate the two systems are in agreement and would provide evidence for the feasibility of upscaling terrestrial structural measures to the scale of aerial lidar. As a secondary outcome, agreement in the two ordination analyses would highlight the capacity of lidar derived structural metrics to define specific forest structural types that could in turn be related to important functional indices. Both analyses were performed using the *vegan* package in R (Oksanen et al. 2019). Data was standardized to account for differences in magnitude and Euclidean distances were used.

1.3 Results

1.3.1 The Influence of Variable Transect Width

Metric values consistently begin to stabilize at a transect width of 10 - 20 meters depending on the site and metric, with many stabilizing at much narrower slice widths (Figure 1.1). The consistency of these results across metrics and sites provides the basis for confidently proceeding with the univariate correlation analysis. The increased metric variation at narrow slice widths is apparent but expected based on the different physical vegetation that would be measured at different random slices in the canopy volume.

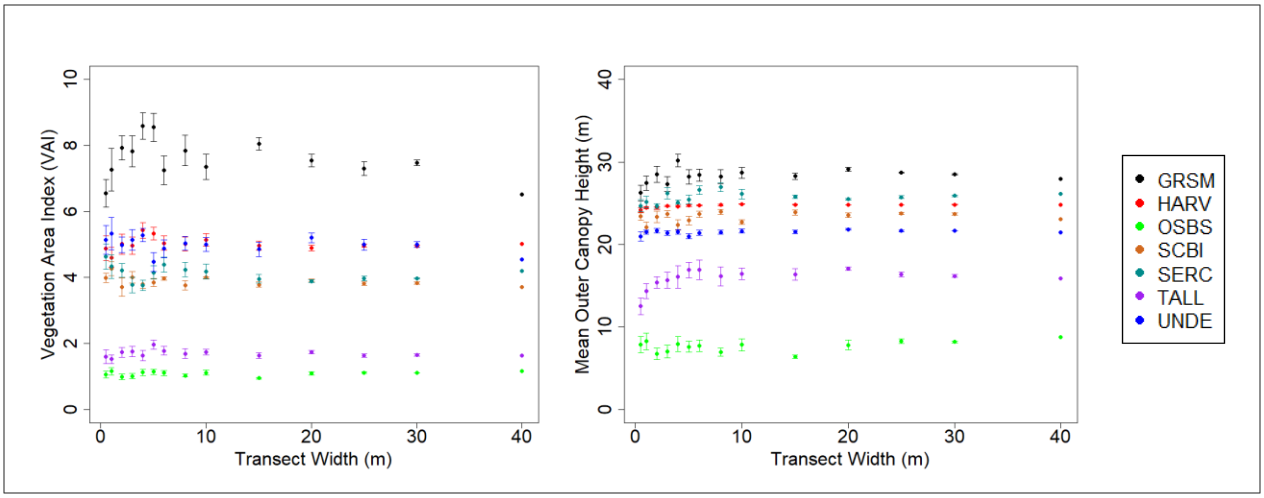

Figure 1.1. The influence of variable derivation area on lidar metric value. Results presented for VAI and mean outer canopy height. Each point represents mean plus standard error for a given transect width. A transect width of 40 m represents the full plot extent. One random plot from each of the seven study sites is represented by each color.

1.3.2 Metric Correlations

The structural metrics exhibited a wide range of correlation coefficients, ranging from *-0.81* to *0.94* (Figure 1.2). Generally, the highest number of correlations had values of $r = 0.5$ - *0.7*, corresponding to the highest peak in Figure 1.2.

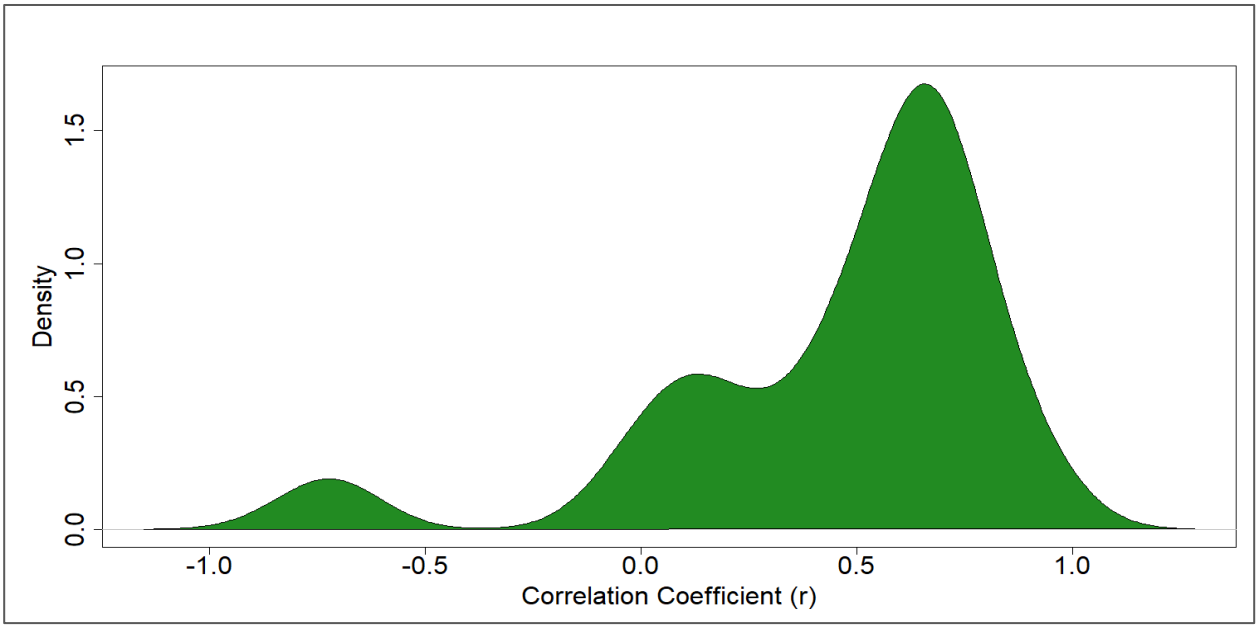

Figure 1.2. Kernel density plot showing the overall distribution of pairwise Pearson's correlation coefficients (*r*) between the aerial and terrestrial metric suites across all metric categories.

However, there is discrepancy between correlation strengths across the four metric categories (Figure 1.3). We see strong correlations in the height category with maximum canopy height (*r = 0.94*) and mean outer canopy height (*r = 0.84*) (Fig. 1.3A). Mean canopy height showed a moderate correlation (*r = 0.68*; Fig. 1.3A). The first peak in the bimodal distribution seen for the height category results from the weak correlation strengths of Max.el (*r = 0.15 - 0.27*; Fig. 1.3A), defined as the mean height of the maximum VAI return in each column along the PCL transect. All other correlations were above *r = 0.56*. Height metrics possessed moderate to strong correlations but were consistently biased slightly towards ALS (Figure 1.4). In the leaf area and density category, mean VAI had strong positive correlations with terrestrial mean VAI (*r = 0.88*) and terrestrial mean peak VAI (*r = 0.85*) (Fig. 1.3B). In the cover and openness category, *r* values ranged from ± *0.69 – 0.81* (Fig. 1.3C) as a result of these metrics being functional inverses of each other, such as gap fraction and cover fraction. Aerial cover and gap fraction had strong correlations with terrestrial sky fraction (*r = -0.72* and *r = 0.81*, respectively; Fig. 1.3C). Deep gap fraction, a

measure of canopy gaps larger than 1 m^2, possessed a strong correlation (*r = 0.70*; Figure 1.3C). Canopy heterogeneity metrics exhibited a wide range of correlation values, ranging from *r = -0.03 - 0.75* (Figure 1.3D). Aerial SD of vertical SD was the most consistently correlated metric within its category (*r = 0.61 – 0.73*; Fig. 1.3D). Other metrics show more variable correlations, such as vertical SD of height (*r = 0.26 – 0.74*; Fig. 1.3D). Some metrics show consistently weak correlations, including aerial rumple (*r = 0.02 – 0.46*; Fig. 1.3D). Aerial and terrestrial rumple were weakly correlated (*r = 0.12*; Fig. 1.3D). Terrestrial rumple was in fact more correlated with other heterogeneity metrics than its aerial counterpart, and exhibited several strong correlations. Aerial and terrestrial top rugosity were also weakly correlated (*r = 0.41*; Fig. 1.3D).

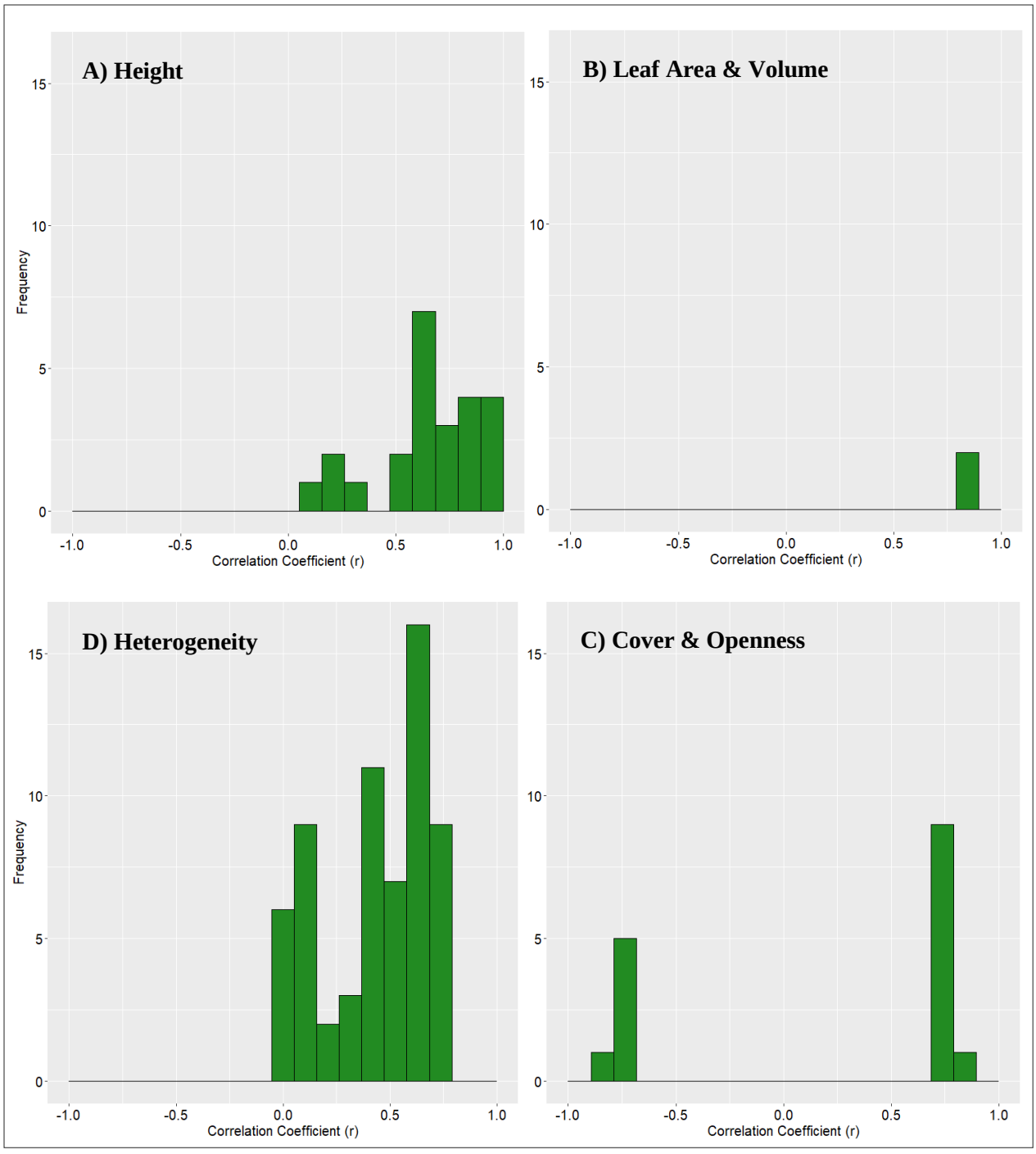

Figure 1.3. Histogram of correlation coefficients for each of the four metric categories. Data presented is across all sites.

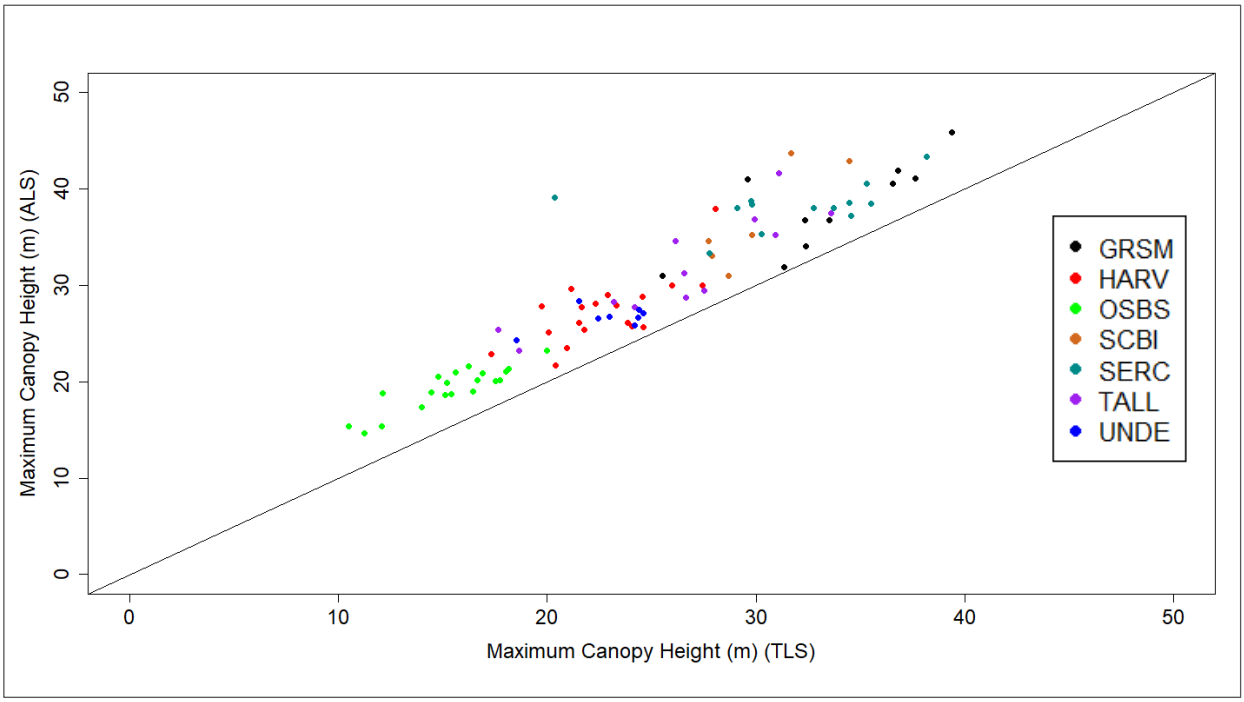

Figure 1.4. Correlation between aerially and terrestrially derived maximum canopy height, showing measurement bias. 1:1 line included. TLS systems tend to underestimate height measures as a result of reduced laser penetration into the upper canopy.

1.3.3 Ordination Agreement of ALS and TLS

Multivariate clustering of the 88 study plots via NMDS illustrates two primary results, the first of which is the comparable ordinations of the aerial and terrestrial metric suites (Figure 1.5). It can be observed that both ordinations produce three clusters containing the same sites, showing that composite measures of structure are in agreement much like many of the univariate structural measures. Not only do the clusters exist in both cases, but they are oriented similarly, further emphasizing system compatibility. Additionally, while perhaps not readily apparent due to the 3-D view presented, each of the seven sites form an individual cluster that is completely separable from the other sites. This relates to the second primary outcome in that composite measures of canopy structure may be able to identify distinct forest structural types (Fahey et al. *in review*) across a heterogeneous landscape.

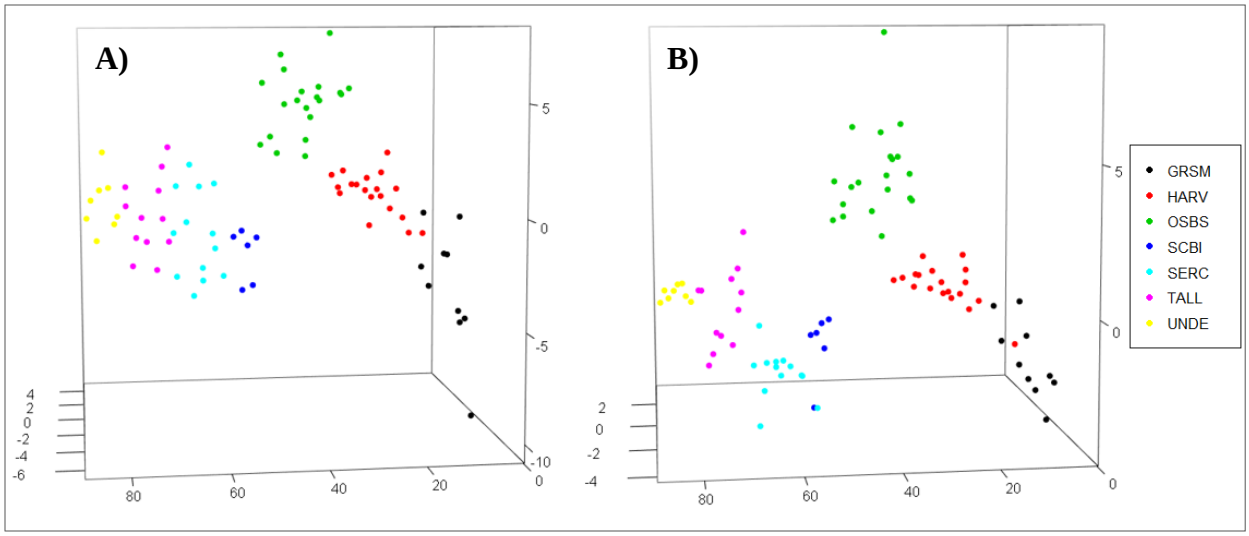

Figure 1.5. Site-level NMDS ordination of A) terrestrial metric suite and B) aerial metric suite. Each point (n=88) represents an individual plot. Each axis represents a composite of multiple metrics to visualize the data in three-dimensional space.

The NMDS ordinations show how the sites compare in multidimensional structural space but do not reveal what, if any, metrics are the driving variables. To this end, the results of the PCA analysis show the contribution of individual structural metrics to the observed clustering (Figure 1.6). For the terrestrial metric suite, the first two principal axes account for over 80% of the observed variability (Figure 1.6A), with many metrics contributing to both. That is, there is not necessarily one singular metric that dominates the others. In fact, metrics from all four categories are important based on Figure 1.6A, with different categories weighing most heavily towards specific sites. Particularly noticeable is the weighting of horizontal cover towards the Ordway-Swisher Biological Station site, a pine savannah ecosystem. We see similar ordination results with the aerial PCA with a number of metrics and categories driving the observed differences (Figure 1.6B). The variance accounted for by the first two axes is similar to the terrestrial suite at just over 80%. Again, we see horizontal cover and openness metrics dominating the ordination of the Ordway-Swisher site.

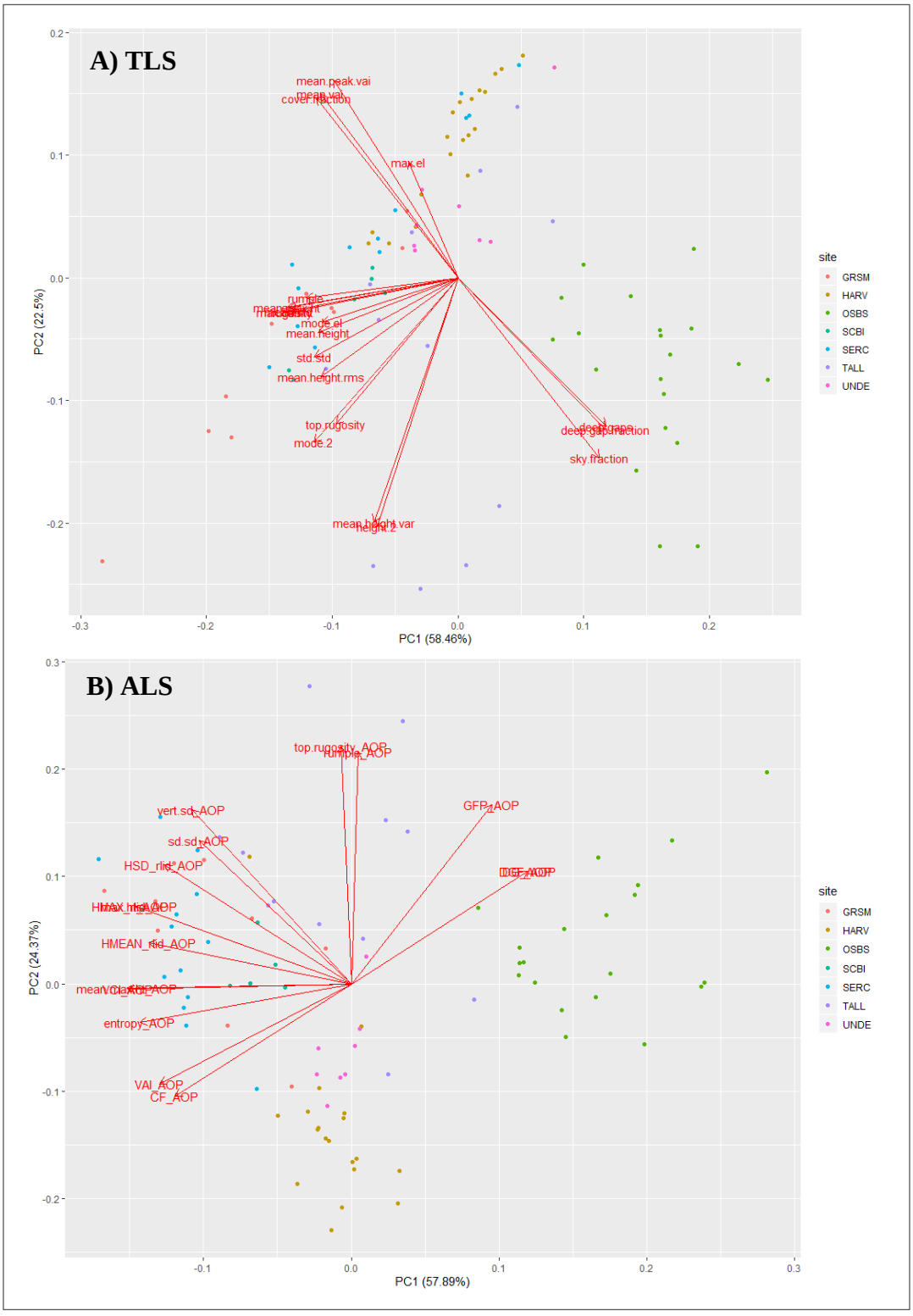

Figure 1.6. PCA ordination of study sites by A) terrestrial metrics and B) aerial metrics. Each point represents an individual plot. Arrows represent the relative contributions of each structural metric to the ordination of the study plots.

1.4 Discussion

1.4.1 Aerial and Terrestrial Lidar Compatibility

There were metrics in all four categories that exhibited strong correlations, but overall, the canopy height, vegetation area and density, and cover and openness categories possessed moderate to strong relationships for all pairwise correlations (except for the Max.el height metric). Our findings show that several important individual measures of forest structure can be feasibly upscaled and applied across heterogeneous landscapes: maximum canopy height, mean outer canopy height, VAI, cover fraction, gap fraction, and deep gap fraction. All of these metrics had strong correlations ($r \geq 0.7$) between their aerial and terrestrial counterpart and all other metrics within their respective category. This assemblage of metrics is a powerful composite combining horizontal structural, vertical structure, and a proxy measure for biomass and productivity. Additionally, mean canopy height and total deep gaps, the raw count of 1 m^2 or larger canopy gaps, were just short of the defined cut-off for a strong correlation ($r = 0.68$ and $r = 0.69$, respectively). Together, univariate structural measures can be related to many important functional measures, especially those related to forest productivity and succession, which are major considerations in the modern world with the ever-present impacts of climate change, land cover change, and invasive species.

We also saw aerial and terrestrial lidar compatibility reinforced by multivariate structural measures. The NMDS ordination illustrated similar clustering of the 88 study plots across multiple scales. First, the ordination produced separate 3-D clusters for each of the seven study sites with both metric suites, showing that the lidar metrics are able to identify and delineate the composite structural attributes that characterize each site. Second, the two ordinations produced three separable clusters, each comprised of the exact same sites, further highlighting the compatibility of the two systems and pointing to similar structural attributes between the sites. Not only are the

observed levels of clustering equivalent between the two ordinations, but the overall distribution of the 88 study plots and 7 sites in structural space is similar. These results show the compatibility of the ALS and TLS systems at the plot, site, and ecosystem levels. Indeed, the clustering makes ecological sense, as well, considering the forest types. The only unexpected result is that Talladega National Forest is not clustered with Ordway-Swisher Biological Station, as these are both pine savannah ecosystems. These sites have similar horizontal structure, and so perhaps other structural attributes are driving the observed differences.

Indeed, this is highlighted in the results of the PCA ordinations, where it is observed that while Ordway-Swisher is heavily weighted by measures of horizontal canopy structure (i.e. cover and gap fraction), Talladega National Forest is oriented more based on measures of canopy complexity, particularly outer canopy roughness (rumple and top rugosity). This suggests that while these sites may be comparable in general horizontal canopy cover, other site characteristics are leading to differences in vertical structure. One possible reason for this is past land use— while Ordway-Swisher has been historically maintained via controlled burning, the Talladega National Forest site was extensively logged and eroded prior to its acquisition in the early 20th century. We also see certain other sites being dominated by individual metrics or a specific metric category, such as Smithsonian Environmental Research Center and Great Smoky Mountain National Park and canopy height metrics. The results of the NMDS and PCA ordinations give evidence to the idea of distinct canopy structural types (Fahey et al. *in review*) in forest ecosystems. Being able to extract structural measurements from lidar that can delineate structural types is a powerful tool for relating those structural measures to known functional characteristics associated with specific forest types. It also further illustrates the potential for measuring canopy structural complexity across broad, heterogeneous landscapes.

The wide range of correlation strengths for heterogeneity metrics, along with the increased number of weak correlations (partly a proxy from the increased number of heterogeneity metrics), indicates that upscaling these metrics to regional and landscape extents remains a challenge. Aerial standard deviation of vertical standard deviation is the only metric that exhibited moderate to strong correlations with all other heterogeneity metrics, although it was not strongly correlated with its terrestrial counterpart. Several factors could be playing into the occurrence of weak to negligible correlations.

One, it could be related to the functional and operational differences of the two lidar systems. While the aerial system collects a point cloud of a full plot extent, the terrestrial data is collected by averaging three walked transects across each plot. This could produce terrestrial data that does not incorporate major structural elements of an individual plot such as a large canopy gap or standing snags, skewing the resulting correlation. Also, aerial data could be influenced by whether or not an individual plot was located near the flight line as opposed to the edge of a scan area, potentially introducing noise into the data. The PCL system collects data in a continuous vertical direction, and so this is not expected to be a factor for the terrestrial data.

Second, it could be attributed to the analytical approach. Separate R packages were used for the aerial and terrestrial metric derivations (*lidR & rLiDAR* and *forestR*, respectively) which could lead to differences that may be exacerbated through the workflow. Moving forward, the abundance of different lidar systems and required workflows is something to be streamlined to facilitate compatible data processing across systems and scales. The results of the heterogeneity correlations, in combination with the other univariate correlations and multivariate ordinations, suggest that as opposed to attempting to characterize canopy complexity by individual metrics, composite measures that holistically characterize a canopy may be more effective.

1.4.2 Measuring Canopy Structure at Large Spatial Extents

Currently, having detailed measures of canopy structure and structural complexity at large spatial scales is a missing piece in ecological studies. This is an advancement that would allow detailed, accurate structural measures to then be applied across areas and in locales where terrestrial data is not readily available or feasible to collect. This is a development that would circumnavigate the time, labor, and financial requirements of terrestrial data collection and lead to more robust ecological models. Structure-function relationships are known to exist and are important to incorporate to ensure models are as comprehensive as possible, and that forest management and conservation strategies are as informed, and in turn effective, as possible. Furthermore, it is an advancement that would open up the door for relating canopy complexity to climate change, in both how climate change impacts canopy structure and how canopy structure influences the effects of climate change.

1.4.3 Conclusion

The objective of this study was to evaluate the compatibility of aerially and terrestrially derived lidar structural measures to establish the basis for upscaling functionally relevant terrestrial structural metrics to the scale of aerial lidar collection. We found that several univariate measures of canopy structure can feasibly be upscaled, including maximum canopy height, mean outer canopy height, vegetation area index, cover fraction, gap fraction, and deep gap fraction. We also showed that the two lidar systems used are in agreement when considering multivariate measures of structure. Moving forward, focus should be put on advancing our capacity to measure the physical 3-D complexity of canopy structure, as results showed shortcomings in the agreement of individual complexity metrics. Perhaps moving towards composite, holistic measures of structure and structural complexity is the way forward. Work such as this will continue to expand the

capabilities of lidar for ecological applications and further refine our understanding of its limitations. Future sustainability requires a comprehensive understanding of our environment and the shifting dynamics of the natural world in the modern age, and lidar is a tool to improve our capacity to do so.

CHAPTER 2. TERRESTRIAL VS UAV LASER SCANNING

2.1 Introduction

2.1.1 Canopy Structure as a Component of Forest Ecosystems

The physical structure of forest ecosystems is an important consideration as it influences many ecological patterns and processes. In particular, the physical structure of forest canopies affects a range of forest functions, including primary production (Hardiman et al. 2011), nutrient cycling and energy transfer (Parker et al. 2004a, Hardiman et al. 2013, Atkins et al. 2018), and habitat provisioning (Bergen et al. 2009). Canopy structure is subject to a wide range of factors including community composition, topography, climate, and edaphic characteristics, meaning canopy structure is often both physically and biotically complex while varying dynamically across both space and time. Structurally complex canopies facilitate more effective absorption of incoming solar radiation through increased transmission and interception of diffuse light throughout the canopy, which plants use more efficiently than direct light (Li et al. 2015). Physical structure therefore plays a critical role in regulating forest carbon cycling, however, these complexities are often omitted or greatly simplified in ecosystem models, potentially limiting the accuracy of estimates of important ecosystem functions (Fisher et al. 2017). Easy and accurate measurements of structural complexity could substantially improve our ability to model important structure-function relationships as well as bolster forest management and conservation strategies. However, many conventional sensors and technologies, such as images collected from passive remote sensing systems, have exhibited shortcomings in measuring canopy structure with increasing aboveground biomass and leaf area index (Lefsky et al. 2002a).

2.1.2 Quantifying Forest Canopy Structure

Lidar (light detection and ranging) can measure three-dimensional canopy structure and has been demonstrated as a means to characterize structure-function relationships (Lefsky et al. 2002b, Lim et al. 2003, Hopkinson et al. 2004, Mascaro et al. 2011, Asner et al. 2012, Yang et al. 2013, Nguyen et al. 2016, Disney et al. 2018, Hardiman et al. 2018, Larue et al. 2018). Terrestrial laser scanning (TLS) can measure internal canopy structure metrics at extremely high resolutions (Hopkinson et al. 2004, Hardiman et al. 2011, Atkins et al. 2018, Almeida et al. 2019), but is limited in its implementation across large spatial extents. Conversely, aerial laser scanning (ALS) can be deployed over wide spatial extents but sacrifices the high data resolution achievable with TLS.

Integrating ALS and TLS would allow accurate measurement of structural dynamics from local to continental scales and provide the capability to scale functionally-relevant local structure to regional and continental scales. Increasingly, lidar data collected via unmanned aerial vehicles (UAVs) have been utilized in ecological studies in an attempt to bridge the tradeoff between TLS resolution and ALS spatial extent (Getzin et al. 2014, Wallace et al. 2016, Guo et al. 2017). UAV systems allow for higher point densities than traditional plane-flown aerial lidar while still retaining the maneuverability and extended spatial capacity. UAV flown systems could prove immensely advantageous for collecting expansive, detailed scans at local to mesoscales as opposed to the numerous individual scans required by TLS. As canopy structure is dynamic both temporally and spatially, UAV systems offer the potential to monitor changes in structure and in turn improve our capacity to model structural dynamics. Conservation strategies increasingly rely on spatial data of land cover and vegetation patterns derived from remotely sensed data products (Bergen et al. 2009) and UAV lidar could aid in developing effective and efficient strategies for specific locales. Furthermore, the applicability of UAV systems could prove valuable for forest managers— while

structural complexity is inherently important in natural forest ecosystems, maximizing productivity is a primary goal for forest plantations and regeneration efforts, and functionally-relevant lidar structural measures could be capitalized on to inform decision making.

2.1.3 Study Objective

Our primary objective was to investigate the relationship between measures of canopy structure derived from UAV and hemispherical scanning terrestrial lidar. Specifically, we aimed to quantify the correlations between a suite of aerially and terrestrially derived structural metrics. Establishing agreement between equivalent structural metrics is a crucial step towards integrating ALS and TLS. If functionally relevant terrestrial measures can be confidently upscaled, we can then apply these measurements across regions and landscapes where terrestrial data is absent or not feasible to collect. Beyond evaluating univariate correlation strengths, we performed structural ordinations using the generated metrics to investigate the efficacy of utilizing multivariate measures to evaluate canopy structure.

2.2 Methods

2.2.1 Study Site

Data was collected from 12-year-old experimental research plots planted at Martell Forest, a research property owned by Purdue University in Tippecanoe County, Indiana. The plots (n=55) are part of a silvicultural trial planted in 2007 to test the effects of interspecific competition and planting density on growth and survival of American Chestnut (Gauthier et al. 2013). Species include American Chestnut (*Castanea dentatea* Marsh.), Black Cherry (*Prunus serotina* Ehrh.), and Northern Red Oak (*Quercus rubra* L.) planted in monoculture treatments (3), two-species mixtures (3), and a three-species mixture (1) for a total of seven unique species composition

treatments. These seven variants are planted in plots with a spacing of 1 m, 2 m, and 3 m between trees, respectively, for a total of 21 unique species-density treatments per block (Figure 2.1A). The site contains a total of 3 blocks (63 plots total), but 8 plots were omitted due to extensive tree mortality.

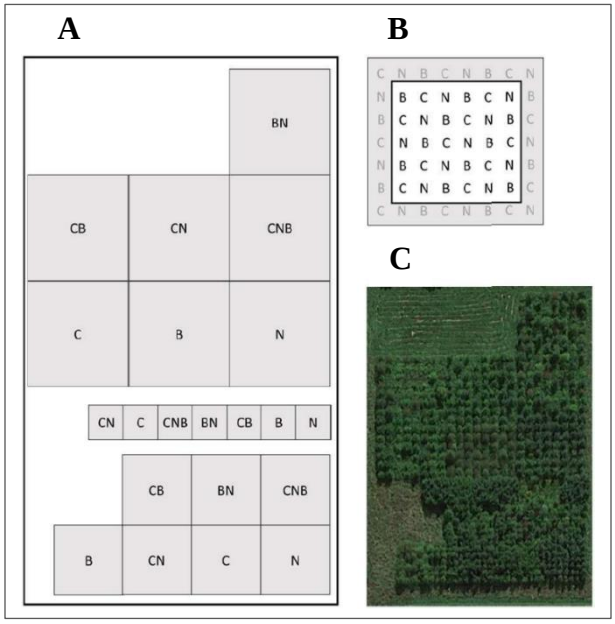

Figure 2.1. Layout of Martell study site. A) Individual block, B) individual plot, C) satellite image of a block. Figure modified from AgSEED research proposal. For blocks and plots, B= Black Cherry, C = American Chestnut, N = Northern Red Oak. 56 trees total per plot.

2.2.2 Data Collection

UAV lidar data was collected during full-leaf out in mid-August, 2018, with a Velodyne VLP-16 system (Table 2.1). TLS data was collected in early September, 2018, with a Leica BLK 360 system (Table 2.1). The TLS system is a tripod-mounted hemispherical scanner. For the purpose of this study, a single scan was collected from the centroid of each plot. A circle of radius 2.5 m was used to calculate structural metrics across all plots. This corresponds to the area of the one-meter spaced plots (additional analysis results using variable radii are included in the Appendix; App. 1.1). A circular area was used to account for misalignment between plot scans,

therefore not incorporating canopy elements from adjacent plots. This was also done to evaluate the ability of a single scan to collect sufficient data because incorporating the full plot extent for the two and three-meter spaced plots (n=34) would require multiple scans per plot, which would substantially increase the labor, time, and computational requirements.

The UAV system was flown over the entire site at an altitude of 50 m with 4.3 m lateral distance between scan lines. To ensure collection height does not substantially impact derived metric values, a scan with the same operational parameters but flown at an altitude of 20 m was also collected. The results of this comparison are included in the Appendix (App. 1.2). There were not significant differences in metric value between the two heights. Therefore, further analysis was performed using the 50 m altitude data, as it is a smaller file size and thus more efficient to work with. Individual plots were clipped from the UAV point cloud using GPS coordinates collected at each plot's centroid with a Trimble R2 GPS unit. In all cases, GPS horizontal accuracy was within 10 cm. Just as with the TLS data, a circle of radius 2.5 m was used for analysis of all 55 plots.

Table 2.1. Lidar system specifications.

System Specifications	Velodyne VLP-16 (UAV)	Leica BLK360 (TLS)
Returns per Pulse	Single/Dual	Single
Wavelength	903 nm	830 nm
Measurement Range	100 m	60 m
Range Accuracy (typical)	± 3 cm	± 4 mm - 7 mm
Measurement Rate (per second)	300,00/600,000	360,000
Average Point Density	~1,000 per m^2 / 100 - 120 per m^3	~300,000 per m^2 / 30,000 - 60,000 per m^3
Laser Product Classification	IEC 60825-1:2007 & 2014 (Eye-safe)	IEC 60825-1:2014 (Eye-safe)

2.2.3 Lidar Structural Metrics

In order to evaluate the correlation strengths between the two systems, a single structural metric suite was generated (Table 2.2). The suite is divided into four metric categories, each

characterizing a different aspect of canopy structure: (1) *canopy height*, (2) *vegetation area and density*, (3) *canopy cover and openness*, and (4) *canopy heterogeneity* (Atkins et al. 2018).

Analyses were performed using the R programming language (The R Group) and the *lidR* and *rLiDAR* R packages (Roussel et al. 2018, Silva et al. 2017). Processing the UAV data requires plot coordinates to clip individual plots from the full site point cloud using the *lidR* package. Some metrics can be derived directly from the 3-D point cloud while others are derived from a canopy height model (CHM) that is created for each study plot. The CHM is generated by rasterizing the point cloud in 1 m^2 pixels and assigning each pixel the value corresponding to the highest lidar return within the corresponding 1 m^2 column of the point cloud. The terrestrial workflow is equivalent to that of the aerial except that each plot is represented by an individual scan and thus the clipping procedure is omitted.

To compare the correlation strength between aerial and terrestrial metrics across the various treatments and metric categories, Pearson correlation coefficients (r) for each within-category (i.e. height vs height metrics) pairwise correlation were evaluated. The multivariate structural ordinations were performed using the *vegan* R package (Oksanen et al. 2019). First, a non-metric multidimensional scaling (NMDS) procedure was performed, using Euclidean distances and 20 maximum iterations. Separate NMDS ordinations were performed for the terrestrial and aerial metrics. The NMDS is designed to reduce the dimensionality of the input data and ordinate the study plots based on their structural attributes. A principle component analysis (PCA) was also performed for the purpose of establishing what structural metrics are driving plot clustering. Input data was standardized to account for differences in magnitude and Euclidean distances were used.

Table 2.2. Lidar structural metric suite. Included is a brief description of each metric— all are equivalent to metrics measured in Chapter 1.

Metric	Category	Description	Unit
Mean Canopy Height	Height	Mean canopy height of point cloud	m
Mean Outer Canopy Height	Height	Mean pixel value of canopy height model (CHM)	m
Maximum Canopy Height	Height	Maximum canopy height in CHM	m
Vegetation Area Index (VAI)	Vegetation	Summation of leaf area density in 1 m layers of point cloud	N/A
Cover Fraction	Cover & Openness	Number of CHM pixels above ground height divided by total number of CHM pixels	0-1
Gap Fraction	Cover & Openness	Number of CHM pixels at ground height divided by total number of CHM pixels	0-1
Gap Fraction Profile	Cover & Openness	Mean gap fraction of 1 m layers in point cloud	0-1
Rumple	Heterogeneity	Ratio of outer canopy surface area to ground surface area	ratio
Top Rugosity	Heterogeneity	Standard deviation of CHM heights	m
Height SD (lidR)	Heterogeneity	Standard deviation of point cloud return heights	m
Height SD (rLiDAR)	Heterogeneity	Standard deviation of point cloud return heights	m
SD of Vertical SD of Height	Heterogeneity	Standard deviation of rasterized standard deviation of point cloud return heights	m

2.3 Results

2.3.1 Terrestrial and UAV Lidar Metric Compatibility

The structural metrics exhibit a wide range of correlation coefficients between equivalent aerial and terrestrial measures (Table 2.3). The three height metrics show moderate ($| r | \geq 0.50$) to strong ($| r | \geq 0.70$) correlations across all treatment considerations, and all height correlations are strong besides for two instances of maximum canopy height (*r = 0.55, r = 0.56*; Table 2.3). Mean outer canopy height exhibits particularly strong correlations, ranging from *r = 0.81 – 0.96* (Table 2.3). VAI shows a wide range of correlation coefficients, but the majority of instances are moderate or higher, with one strong correlation (*r = 0.73*; Table 2.3). The two weak correlations correspond to the collection of non-monoculture treatments. The cover and openness metrics (gap fraction, cover fraction, and gap fraction profile) show consistently weak ($| r | < 0.50$) correlations. Gap and cover fraction are moderately correlated when considering the treatment plots with three species (*r = -0.65;* Table 2.3). The occurrence of negative correlations between equivalent metrics is an unexpected result. Gap fraction profile shows a similar pattern, showing both a positive moderate correlation (*r = 0.62*; Table 2.3) and negative moderate correlation (*r = -0.53*; Table 2.3) across two species richness treatments. The occurrence of unexpected negative correlations carries over into the heterogeneity metrics, as well. All metrics beside top rugosity exhibit both positive and negative correlations between aerial and terrestrial counterparts. Besides for one instance, top rugosity exhibits consistent moderate to strong correlations (*r = 0.62 – 0.82*; Table 2.3). Vertical standard deviation of height, too, shows some strong correlations, but these are unexpected in their directionality.

Table 2.3. Pearson's correlation coefficients (r) across treatments for each of the 12 lidar structural metrics. Data presented are correlation coefficients between aerial and terrestrial counterparts of equivalent metrics.

	Spacing Treatment			Species Richness Treatment		
Metric	1 m	2 m	3 m	1	2	3
Mean Outer Canopy Height	0.95	0.9	0.81	0.96	0.89	0.95
Maximum Canopy Height	0.56	0.95	0.55	0.79	0.74	0.9
Mean Canopy Height	0.82	0.80	0.76	0.91	0.84	0.86
Vegetation Area Index (VAI)	0.57	0.51	0.66	0.73	0.10	0.15
Gap Fraction	0.27	0.05	-0.37	-0.05	-0.12	-0.65
Cover Fraction	0.27	0.06	-0.37	-0.05	-0.12	-0.65
Gap Fraction Profile	0.35	-0.39	0.34	0.62	-0.53	0.11
Rumple	0.55	-0.36	0.42	0.47	0.15	-0.24
Top Rugosity	0.82	0.29	0.68	0.77	0.62	0.76
Vertical SD of Height	-0.75	-0.83	0.08	-0.68	-0.57	-0.32
SD of Vertical SD of Height	0.31	-0.34	0.81	0.48	-0.23	-0.11
Height SD	-0.49	-0.19	0.66	-0.10	-0.53	-0.42

Results of the NMDS analysis show no noticeable clustering across biodiversity and species richness treatments (Figure 2.2A). However, there are distinct groupings that form when the plots are presented by stem density (Figure 2.2B). For both ordinations it can be observed that there is complete clustering out of each of the unique stem density treatments. The treatments are also oriented similarly between the two ordinations. This is more readily apparent if outlier plots are ignored. It can also be seen that each stem density treatment occupies a large space within the NMDS ordination, suggesting structural variation within each treatment (Figure 2.2B).

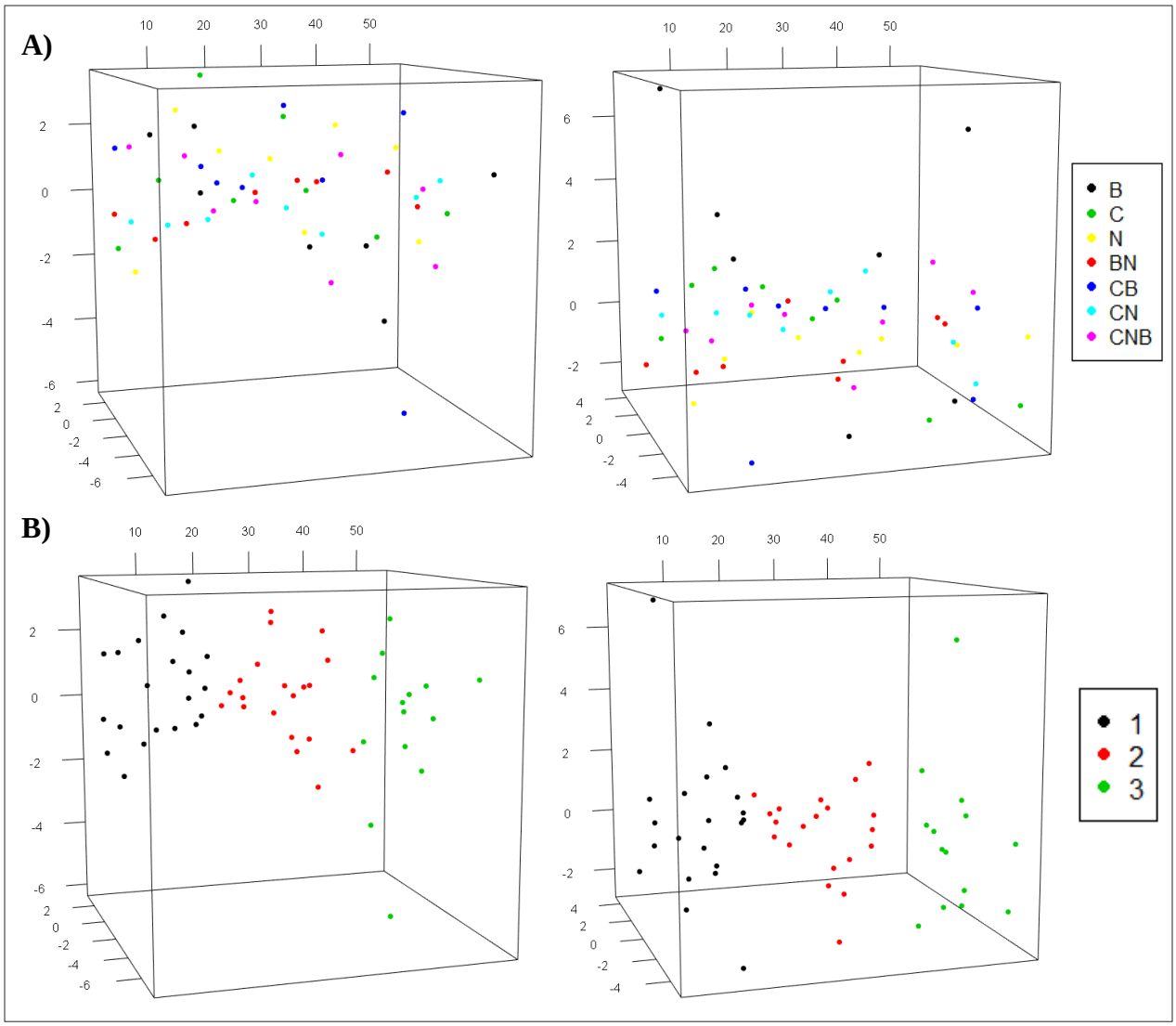

Figure 2.2. NMDS ordination of study plots by A) biodiversity and B) stem density treatments, with aerial metrics on the left and terrestrial metrics on the right. Each point represents an individual plot and each color represents a treatment. The axes carry no explicit ecological meaning beyond their utility to ordinate the plots in space.

Beyond the NMDS ordination, we performed a PCA analysis to identify what, if any, structural metrics are most influential across the various treatments (Figure 2.3). Presented by the three spacing treatments, we see a general separation between the three-meter spaced plots and the one and two-meter spaced plots, although it is not perfect due to the 2-D presentation. This is the

case for both the UAV and TLS ordinations. It can be seen that the one and two-meter spaced plots are dominated in both cases by measures of canopy height. This is especially true for the aerial ordination, where we also see VAI having substantial loading. The three-meter spaced plots are influenced more by measures of canopy structural heterogeneity for the UAV ordination. In the terrestrial ordination we see the majority of structural metrics weighted towards the one and two-meter spaced plots, with the three-meter plots not being substantially influenced by any specific metric. Combined, the first two PCA axes account for over 70% of the observed variation among the plots in both ordinations. We see the first axis accounting for more variability in the aerial ordination than the terrestrial (56.34% vs 46.97%).

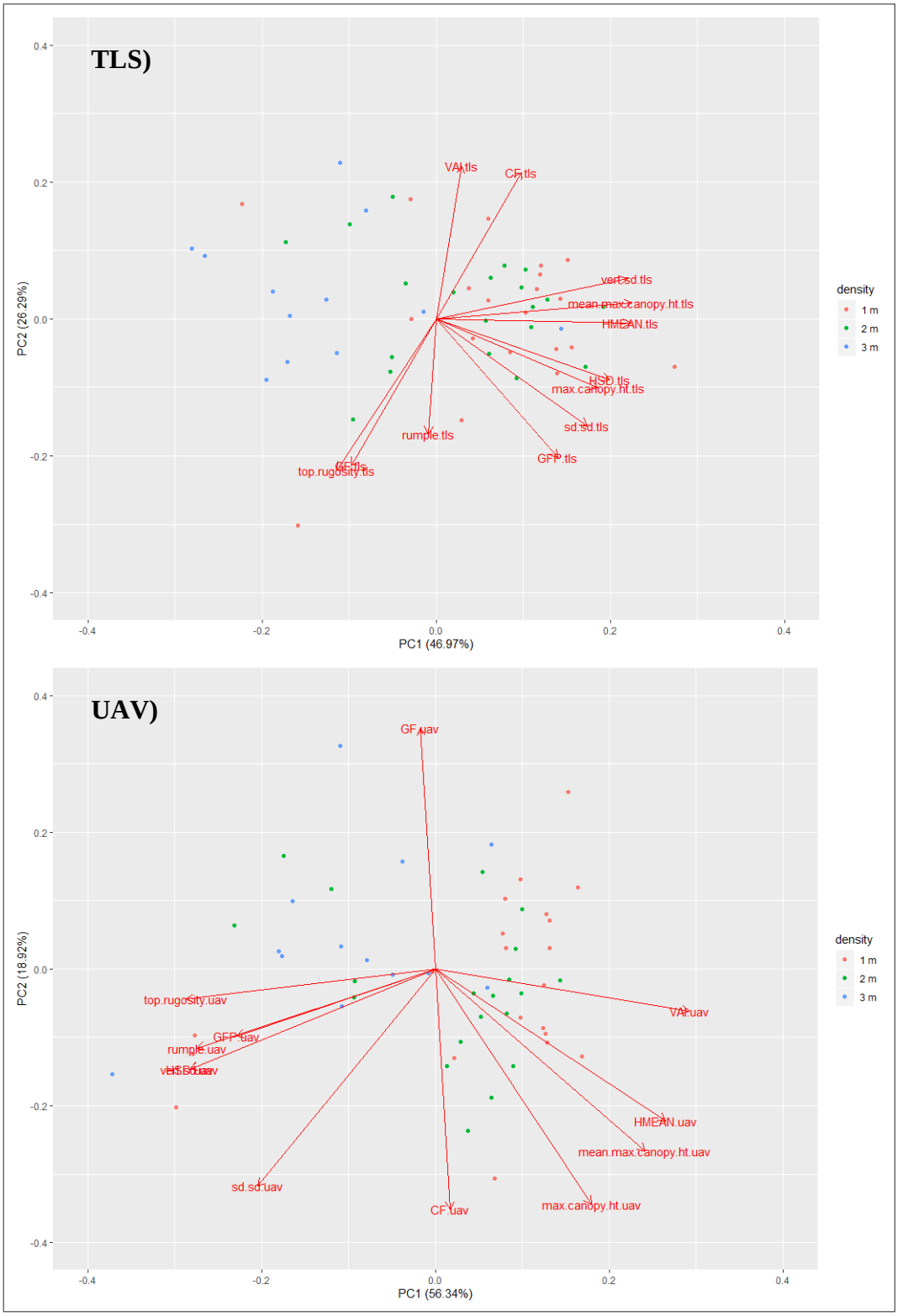

Figure 2.3. PCA ordination of the 55 study plots, presented by spacing treatment. Each point represents an individual plot. The arrows correspond to individual structural metrics, with their relative length corresponding to their relative loading.

2.4 Discussion

2.4.1 Upscaling Lidar Structural Metrics

First considering the univariate correlation analysis, the results suggest the feasibility of upscaling measures of mean outer canopy height, maximum canopy height, mean canopy height, VAI, and top rugosity to the spatial extent of UAV lidar collection. Mean canopy height and mean outer canopy height have strong correlations across all instances that were examined, instilling particular confidence in these metrics. Maximum canopy height also exhibits strong correlations except for in the one and three-meter spaced plots. The moderate correlation ($r = 0.56$) observed for the one-meter spaced plots could be a result of the very dense nature of these plots, leading to reduced laser penetration into the upper canopy. As maximum canopy height is a measure of the single tallest canopy element, increased optical occlusion could lead to a failure of TLS to measure that specific element at a given plot. Conversely, the outer canopy is the first surface that the UAV system measures, and so maximum canopy height measures would be expected to be very accurate.

VAI shows moderate to strong correlations across four of the treatment levels considered, suggesting the feasibility of upscaling measures of vegetation area. Two weak correlations ($r = 0.10, r = 0.15$) were observed for the plots with multiple species present. This is potentially again related to the functional differences between terrestrial and aerially flown lidar systems. The presence of multiple species in a plot might be expected to lead to more complex structure than a monoculture treatment, thus exacerbating the influence of optical occlusion resulting from the alternative viewpoints.

Based on the results showing a consistent lack of moderate or strong correlations among the cover and openness metrics, there is a lack of compatibility between the hemispherical scanning terrestrial system and the UAV operated system for measuring canopy cover and

openness. The occurrence of negative correlations between equivalent metrics particularly emphasizes this. It is likely that the functional differences of the two systems again influence this, but can more likely be attributed to differences in view directionality than the simple fact that one is a terrestrial system and the other is aerial. While the UAV system collects data in a predominately vertical fashion, the TLS system collects data from a centralized location from which pulses are emitted in all 360°. As the cover and openness metrics characterize horizontal structure across a landscape, these metrics favor the collection method of the UAV system. The cover and gap fractions measured by the terrestrial system will be inherently influenced by optical occlusion and also its ability to capture extremely high-resolution structure, which could lead to actual gaps not being identified as such.

We see similar results regarding negative and weak to negligible correlations in the heterogeneity category, as well. Again, these relationships are likely resulting from the functional and operational differences of the two lidar systems. Another plausible factor is the difference in collected point density. Terrestrial lidar systems such as the one utilized in this study are able to achieve remarkably high point densities, a fact that could introduce noise into an analysis when attempting to make comparisons to a system that produces data with point densities that are multiple magnitudes lower. Despite this, top rugosity, a measure of outer canopy surface roughness, displayed moderate to strong correlations in five out of the six treatment levels considered. This suggests the feasibility for upscaling this measure to the scale of UAV systems. Top rugosity is a direct measure of outer canopy complexity that can be related to many attributes and functions of forests, including species composition, successional stage, productivity, and habitat suitability. A measure such as top rugosity, in combination with the other univariate measures highlighted as feasible for upscaling (height metrics and VAI), is a powerful composite for investigating

structure-function relationships, and especially for forest managers who desire to quantify productivity and other important characteristics.

There are several other considerations that could be influencing the specific correlation coefficients that were observed. One, non-treatment woody species have established throughout the Martell Forest site and are either growing among the planted trees or have supplanted treatment species. This leads to increased instances of optical occlusion for the terrestrial data, which has implications for point density and overall data collection and quality. The results of this study also suggest that a single centralized scan may not be sufficient for adequately measuring canopy structure in increasingly large forest stands. Although not feasible for this particular study, combining multiple scans for each individual plot may have illustrated more consistent correlations. Lastly related to the univariate structural measures, the same computational packages were used to evaluate both an aerial and terrestrial lidar metric suite. This could perhaps lead to inherent differences that are difficult to tease apart without knowing the internal workings of a computational package, in the sense that the aerial and terrestrial scans are 'seen differently'.

The results of the NMDS ordination also offer evidence to support the compatibility of the UAV and TLS systems, giving credence to the pursuit of upscaling terrestrial metrics. While there was no apparent clustering across the biodiversity treatments, there was distinct clustering for the three stem density treatments across both the UAV and TLS metric suites. Not only do they independently cluster, but the similar clustering between the two suites suggests the systems are seeing the plots similarly when considering multivariate structure, giving evidence to the feasibility of upscaling multivariate structural measures. These results also highlight the potential for lidar to be used in classifying forest structural types across heterogeneous landscapes (Fahey et al. *in review*), and reinforces our findings from the first chapter of this thesis, where we saw

similar results in natural forest ecosystems across the eastern United States. Being able to categorize forest communities based on structural attributes is a powerful tool, as 3-D forest structure is intimately linked to forest functioning.

The PCA analysis highlights what specific structural metrics are driving the observed clustering in the NMDS ordination, giving further evidence to the ability of lidar derived structural metrics to identify and delineate distinct structural types. The fact that these observations were made for both the terrestrial and UAV PCA ordinations again lends evidence to the compatibility of the two systems, providing grounds for confidently upscaling terrestrial measures to the spatial extent achievable with UAV.

2.4.2 Conclusions

The purpose of this study was to investigate the relationship between a suite of lidar metrics derived from UAV and terrestrial hemispherical scanning systems to establish the feasibility for upscaling functionally-relevant terrestrial structural measures. Our results showed agreement between terrestrial and aerial measures of mean outer canopy height, maximum canopy height, mean canopy height, VAI, and top rugosity, specifically, as well as agreement between multivariate structural measures. The ability to measure canopy structure in detail at large spatial extents is currently a missing component of ecological studies and would substantially improve ecological modeling.

Specifically, the increased data resolution of UAV lidar relative to traditional ALS systems, along with its maneuverability, suggest that these systems could prove monumental in being able to monitor and measure local to mesoscale canopy dynamics, both spatially and temporally, such as throughout individual growing seasons. These benefits make it an attractive tool for forest

managers and land owners to make use of for quantifying and monitoring structure and its influence on forest productivity. We recommend UAV lidar for applications such as these as it eliminates the need for many terrestrial scans to be collected and joined, which is labor, time, and resource intensive. UAV lidar is also much more readily available compared to the logistics and preparations that must be made for plane-flown lidar missions. Integrating lidar-derived 3-D structural metrics in ecological modeling, forest management, and conservation strategizing is an important step to ensure that our understanding of forest dynamics and resulting implementations are as robust and effective as possible so as to best ensure the sustenance of our planet's forest ecosystems.

CHAPTER 3. CONCLUSION

This thesis was undergone with the purpose of establishing the grounds for the feasibility of upscaling functionally-relevant local scale structural measures to the spatial extents that are achievable with aerial lidar systems. Forest structure, and specifically canopy structure, is known to be an important factor that influences many ecosystem functions, particularly productivity. However, three-dimensional canopy structure can be challenging to characterize by passive remote sensing technologies and traditional forest inventory techniques due to its complex and dynamic nature. As a result, it is often oversimplified or not incorporated in ecological models. We therefore commonly make use of estimations and quantifications that are not comprehensive and in turn may be skewed or outright incorrect. Incorporating descriptive, accurate, 3-D measures of canopy structure across heterogeneous landscapes would serve a number of fronts, including more robust ecological modeling, informed forest management, and effective conservation strategies.

Terrestrial lidar systems have been shown to be effective in quantifying functionally-relevant, local scale measures of 3-D structure. However, it is not realistic to collect terrestrial data across large, heterogeneous landscapes. To this end, it is important to instill confidence in being able to accurately measure structural complexity using aerial lidar systems. This would in turn allow structural measures to be applied across large spatial extents where terrestrial data is not available or feasible to collect.

Our work has illustrated compatibility between equivalent terrestrial and aerial univariate structural measures, including mean canopy height, maximum canopy height, mean outer canopy height, vegetation area index, cover fraction, gap and deep gap fraction, and top rugosity. Together, this collection represents a powerful composite that includes measures of vertical and horizontal structure, biomass, and structural complexity. These are metrics with known relationships to

important forest attributes and functions, such as productivity, succession, habitat provisioning, and nutrient cycling. Upscaling these measures to be applied across heterogeneous landscapes would provide previously untapped insight into the relationship between structure and function. We also highlight agreement between terrestrial and aerial lidar when considering multivariate measures of structure. In fact, the multivariate agreement illustrated in both chapters suggests that, moving forward, multivariate structural measures (or composites of univariate measures) may be more effective to apply from local to continental scales. Furthermore, results suggest the legitimate use of lidar derived structural measures for identifying forest structural types across heterogeneous landscapes.

Moving forward, building upon these findings and refining and developing these capabilities will be an important pursuit to advance the utilization of lidar systems in ecological applications. It is a dynamic tool that can be applied across a range of spatial scales and provides key benefits compared to more traditional techniques for quantifying forest structure. In the modern world, with anthropogenic factors influencing every facet of ecosystem functioning in previously unknown ways, it is imperative that we are able to most fully capitalize on the tools we have at our disposal to understand and monitor the natural world, and lidar is one such tool that has exhibited a wealth of promise.

APPENDIX

Appendix 1.1. Comparison of metric means across stem density treatments using variable derivation areas. For the primary correlation analysis for Chapter 2, a 2.5 m radius circle was used for metric derivations for all 55 study plots, equivalent to the extent of a one-meter spaced plot and chosen to account for edge effect with adjacent plots. Here, radii of 5 m and 7.5 m are used, in addition, corresponding to the extents of the two-meter and three-meter spaced plots, respectively. Data is presented as stem density rather than tree spacing. Species codes are B = Black Cherry, C = American Chestnut, N = Northern Red Oak.

		Mean Outer Canopy Height			Maximum Canopy Height			Vegetation Area Index (VAI)			Gap Fraction			Cover Fraction			Gap Fraction Profile			Rumple			Top Rugosity			Vertical SD of Height			SD of Vertical SD of Height		
Stems / m^2	Sp.	2.5 m	5 m	7.5 m	2.5 m	5 m	7.5 m	2.5 m	5 m	7.5 m	2.5 m	5 m	7.5 m	2.5 m	5 m	7.5 m	2.5 m	5 m	7.5 m	2.5 m	5 m	7.5 m	2.5 m	5 m	7.5 m	2.5 m	5 m	7.5 m	2.5 m	5 m	7.5 m
1.5	B	5.41			10.45			0.235			0.003			0.997			0.983			4.60			1.846			1.191			0.682		
1.5	C	8.41			10.59			0.383			0.003			0.997			0.975			4.66			1.127			2.011			0.685		
1.5	N	7.45			9.10			0.418			0.003			0.997			0.969			3.39			0.969			1.765			0.665		
1.5	BN	7.84			9.33			0.402			0.003			0.997			0.973			2.98			0.783			1.978			0.633		
1.5	CB	6.94			9.85			0.442			0.003			0.997			0.966			4.75			1.300			1.546			0.591		
1.5	CN	7.89			10.11			0.410			0.003			0.997			0.971			4.16			1.028			1.886			0.694		
1.5	CNB	7.56			9.92			0.377			0.003			0.997			0.972			4.43			0.984			1.705			0.617		
0.38	B	5.66	4.93		7.07	7.69		0.223	0.287		0.003	0.001		0.997	0.999		0.971	0.966		3.23	4.37		1.085	1.547		1.061	1.150		0.468	0.552	
0.38	C	8.49	8.30		10.56	10.98		0.361	0.541		0.003	0.001		0.997	0.999		0.978	0.968		4.29	4.50		0.892	1.049		2.010	2.285		0.700	0.669	
0.38	N	7.19	7.15		9.83	10.23		0.422	0.575		0.003	0.001		0.997	0.999		0.973	0.964		3.55	3.56		0.977	0.900		1.814	2.003		0.557	0.552	
0.38	BN	6.57	6.76		8.71	10.21		0.375	0.546		0.003	0.001		0.997	0.999		0.972	0.966		3.61	3.59		1.071	1.078		1.612	1.831		0.543	0.513	
0.38	CB	7.59	7.54		10.01	10.61		0.418	0.583		0.003	0.001		0.997	0.999		0.973	0.963		4.67	4.69		1.085	1.286		1.745	1.953		0.599	0.582	
0.38	CN	7.73	7.57		10.16	10.35		0.403	0.567		0.003	0.001		0.997	0.999		0.975	0.967		4.48	4.20		1.105	1.064		1.820	2.058		0.685	0.611	
0.38	CNB	7.21	7.12		9.55	9.96		0.427	0.582		0.003	0.001		0.997	0.999		0.972	0.964		4.18	4.22		1.090	1.134		1.725	1.913		0.535	0.564	
0.17	B	5.24	4.95	4.63	8.31	9.37	9.42	0.261	0.305	0.327	0.003	0.001	0.000	0.997	0.999	1.000	0.972	0.971	0.969	5.34	5.38	5.35	1.665	1.888	1.944	0.922	1.033	1.085	0.507	0.597	0.636
0.17	C	5.11	5.08	4.88	7.37	8.64	9.05	0.408	0.494	0.529	0.003	0.001	0.000	0.997	0.999	1.000	0.955	0.955	0.955	4.14	4.51	4.94	1.171	1.445	1.542	1.111	1.198	1.234	0.414	0.481	0.521
0.17	N	5.72	5.95	5.74	7.59	8.82	8.83	0.440	0.579	0.633	0.003	0.001	0.000	0.997	0.999	1.000	0.964	0.959	0.955	3.32	3.62	4.12	1.112	1.078	1.296	1.363	1.532	1.581	0.489	0.493	0.555
0.17	BN	5.93	5.56	5.22	8.55	9.09	9.38	0.399	0.502	0.554	0.003	0.001	0.000	0.997	0.999	1.000	0.971	0.965	0.962	4.08	4.45	4.67	1.408	1.578	1.616	1.345	1.465	1.513	0.533	0.535	0.572
0.17	CB	5.49	5.11	4.74	8.75	9.20	9.49	0.392	0.453	0.473	0.003	0.001	0.000	0.997	0.999	1.000	0.963	0.961	0.961	4.71	5.28	5.44	1.270	1.715	1.889	1.028	1.125	1.158	0.407	0.505	0.577
0.17	CN	5.80	5.86	5.73	8.10	9.98	9.98	0.428	0.548	0.597	0.003	0.001	0.000	0.997	0.999	1.000	0.967	0.967	0.964	4.01	4.74	4.91	1.193	1.499	1.516	1.282	1.451	1.504	0.445	0.515	0.549
0.17	CNB	6.13	5.90	5.80	9.37	9.63	10.10	0.341	0.465	0.522	0.003	0.001	0.000	0.997	0.999	1.000	0.975	0.967	0.966	4.77	4.48	4.74	1.567	1.604	1.791	1.508	1.657	1.715	0.569	0.604	0.630

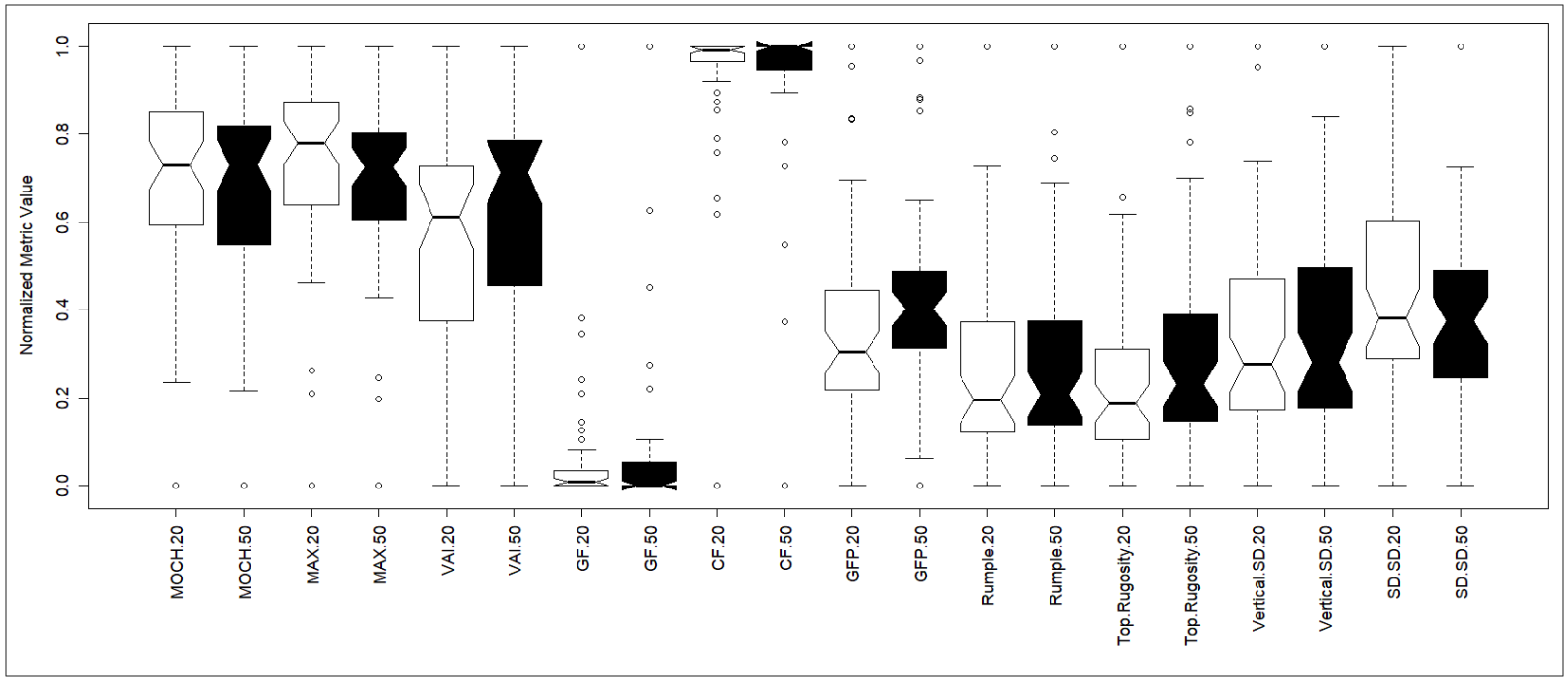

Appendix 1.2. Boxplot comparing UAV collected structural metric values from alternative collection altitudes. White denotes metrics derived from a 20 m flying altitude and black denotes metrics derived from a 50 m flying altitude as indicated on the x-axis. Metric values have been normalized from 0-1 on the y-axis to improve presentation. Acronyms are as follows: MOCH = mean outer canopy height, MAX = maximum canopy height, VAI = vegetation area index, GF = gap fraction, CF = cover fraction, GFP = gap fraction profile, Rumple = rumple, Top.Rugosity = top rugosity, Vertical.SD = Height SD, SD.SD = SD of Vertical SD of Height. Boxes represent the interquartile range, inflection points represent the median, notches represent the 95% confidence interval of the median, whiskers represent the upper and lower quartiles, respectively, and points represent outliers.

REFERENCES

Almeida, D. R. A., Stark, S. C., Chazdon, R., Nelson, B. W., Cesar, R. G., Meli, P., Brancalion, P. H. S. (2019). The effectiveness of lidar remote sensing for monitoring forest cover attributes and landscape restoration. *Forest Ecology and Management, 438,* 34–43. https://doi.org/10.1016/j.foreco.2019.02.002

Asner, G. P., Mascaro, J., Muller-Landau, H. C., Vieilledent, G., Vaudry, R., Rasamoelina, M., van Breugel, M. (2012). A universal airborne LiDAR approach for tropical forest carbon mapping. *Oecologia*, *168*(4), 1147–1160. https://doi.org/10.1007/s00442-011-2165-z

Atkins, J. W., Bohrer, G., Fahey, R. T., Hardiman, B. S., Morin, T. H., Stovall, A. E. L., Gough, C. M. (2018). Quantifying vegetation and canopy structural complexity from terrestrial LiDAR data using the forestr r package. *Methods in Ecology and Evolution*, *9*(10), 2057–2066. https://doi.org/10.1111/2041-210X.13061

Atkins, J. W., Bohrer, G., Fahey, R. T., Hardiman, B. S., Gough, C. M., Morin, T. H., Stovall, A., Zimmerman, N. (2018). Forestr: ecosystem and canopy structural complexity metrics from LiDAR. R package version 1.0.1.

Bergen, K. M., Goetz, S. J., Dubayah, R. O., Henebry, G. M., Hunsaker, C. T., Imhoff, M. L., Radeloff, V. C. (2009). Remote sensing of vegetation 3-D structure for biodiversity and habitat: Review and implications for lidar and radar spaceborne missions. *Journal of Geophysical Research: Biogeosciences 114*(4), 1-13. https://doi.org/10.1029/2008JG000883

Disney, M. I., Boni Vicari, M., Burt, A., Calders, K., Lewis, S. L., Raumonen, P., & Wilkes, P. (2018). Weighing trees with lasers: advances, challenges and opportunities. *Interface Focus*, *8*(2), 20170048. https://doi.org/10.1098/rsfs.2017.0048

Fahey, R.T., Alveshere, B.C., Burton, J.I., D'Amato, A.W., Dickinson, Y.L., Keeton, W.S., Kern, C.C., Larson, A.J., Palik, B.J., Puettmann, K.J., Saunders, M.R., Webster, C.R., Atkins, J.W., Gough, C.M., Hardiman, B.S. (2018). Shifting conceptions of complexity in forest management and silviculture. *Forest Ecology and Management 421*, 59-71. https://doi.org/10.1016/j.foreco.2018.01.011

Fisher, R. A., Koven, C. D., Anderegg, W. R. L., Christoffersen, B. O., Dietze, M. C., Farrior, C. E., Moorcroft, P. R. (2018). Vegetation demographics in Earth System Models: A review of progress and priorities. *Global Change Biology*, *24*(1), 35–54. https://doi.org/10.1111/gcb.13910

Fotis, A. T., Morin, T. H., Fahey, R. T., Hardiman, B. S., Bohrer, G., & Curtis, P. S. (2018). Forest structure in space and time: Biotic and abiotic determinants of canopy complexity and their effects on net primary productivity. *Agricultural and Forest Meteorology*, *250–251*, 181–191. https://doi.org/10.1016/j.agrformet.2017.12.251

Getzin, S., Nuske, R.S., Wiegand, K. (2014). Using Unmanned Aerial Vehicles (UAV) to quantify spatial gap patterns in forests. *Remote Sensing 6,* 6988-7004. https://www.mdpi.com/2072-4292/6/8/6988

Guo, Q., Su, Y., Hu, T., Zhao, X., Wu, F., Li, Y., Liu, J., Chen, L., Xu, G., Lin, G., Zheng, Y., Lin, Y., Mi, X., Fei, L., Wang, X. (2017). An integrated UAV-borne lidar system for 3D habitat mapping in three forest ecosystems across China. *International Journal of Remote Sensing, 38*(8-10), 2954-2972. https://doi.org/10.1080/01431161.2017.1285083

Hardiman, B. S., Bohrer, G., Gough, C. M., Vogel, C. S., Curtis. (2011). The role of canopy structural complexity in wood net primary production of a maturing northern deciduous forest. *Ecology*, *92*(9), 1818–1827. https://doi.org/10.1890/10-2192.1

Hardiman, B. S., Gough, C. M., Halperin, A., Hofmeister, K. L., Nave, L. E., Bohrer, G., & Curtis, P. S. (2013). Maintaining high rates of carbon storage in old forests: A mechanism linking canopy structure to forest function. *Forest Ecology and Management*, *298*, 111–119. https://doi.org/10.1016/j.foreco.2013.02.031

Hardiman, B. S., LaRue, E. A., Atkins, J. W., Fahey, R. T., Wagner, F. W., Gough, C. M. (2018). Spatial variation in canopy structure across forest landscapes. *Forests*, *9*(8), 474. https://doi.org/10.3390/f9080474

Hilker, T., Coops, N.C., Newnham, G.J., van Leeuwen, M., Wulder, M.A., Stewart, J., Culvenor, D.S. (2012). Comparison of terrestrial and airborne LiDAR in describing stand structure of a thinned lodgepole pine forest. *Journal of Forestry*, *110*(2), 97–104. https://doi.org/10.5849/jof.11-003

Hilker, T., van Leeuwen, M., Coops, N.C., Wulder, M.A., Newnham, G.J., Jupp, D.L.B., Culvenor, D.S. (2010). Comparing canopy metrics derived from terrestrial and airborne laser scanning in a Douglas-fir dominated forest stand. *Trees - Structure and Function*, *24*(5), 819–832. https://doi.org/10.1007/s00468-010-0452-7

Hopkinson, C., Chasmer, L., Young-Pow, C., Treitz, P. (2004). Assessing forest metrics with a ground-based scanning lidar. *Canadian Journal of Forest Research*, *34*(3), 573–583. https://doi.org/10.1139/x03-225

Hopkinson, C., Lovell, J., Chasmer, L., Jupp, D., Kljun, N., & van Gorsel, E. (2013). Integrating terrestrial and airborne lidar to calibrate a 3D canopy model of effective leaf area index. *Remote Sensing of Environment*, *136*, 301–314. https://doi.org/10.1016/j.rse.2013.05.012

Gauthier, M.M., Zellers, K.E., Lof, M., Jacobs, D.F. (2013). Inter- and intra-specific competitiveness of plantation-grown American chestnut (Castantea dentata). *Forest Ecology and Management 291,* 289-299. https://doi.org/10.1016/j.foreco.2012.11.014

LaRue, E. A., Atkins, J. W., Dahlin, K., Fahey, R., Fei, S., Gough, C., Hardiman, B. S. (2018). Linking Landsat to terrestrial LiDAR: Vegetation metrics of forest greenness are correlated with canopy structural complexity. *International Journal of Applied Earth Observation and Geoinformation*, *73*, 420–427. https://doi.org/10.1016/j.jag.2018.07.001

Lefsky, M A, Cohen, W. B., Harding, D. J., Parker, G. G., Acker, S. A., & Gower, S. T. (2002). Lidar remote sensing of above-ground biomass in three biomes. *Global Ecology and Biogeography*, *11*(5), 393–399. https://doi.org/10.1046/j.1466-822x.2002.00303.x

Lefsky, Michael A, Cohen, W. B., Parker, G. G., & Harding, D. J. (2002). Lidar remote sensing for ecosystem studies. *Bioscience*, *52*(1), 19–30. https://doi.org/10.1641/0006-3568(2002)052

Li, T., & Yang, Q. (2015). Advantages of diffuse light for horticultural production and perspectives for further research. *Frontiers in Plant Science*, *6*, 1–5. https://doi.org/10.3389/fpls.2015.00704

Lim, K., Treitz, P., Wulder, M., St-Onge, B., Flood, M. (2003). LiDAR remote sensing of forest structure. *Progress in Physical Geography: Earth and Environment*, *1*, 88–106. https://doi.org/10.1191/0309133303pp360ra.

Listopad, C.M.C.S., Drake, J.B., Masters, R.E., Weishampel, J.F. (2011). Portable and airborne small footprint LiDAR: Forest canopy structure estimation of fire managed plots. *Remote Sensing*, *3*(7), 1284–1307. https://doi.org/10.3390/rs3071284

Mascaro, J., Detto, M., Asner, G. P., Muller-Landau, H.C. (2011). Evaluating uncertainty in mapping forest carbon with airborne LiDAR. *Remote Sensing of Environment, 115*(12), 3770–3774. https://doi.org/10.1016/j.rse.2011.07.019

Nguyen, H.T., Hutyra, L.R., Hardiman, B.S., Raciti, S.M. (2016). Characterizing forest structure variations across an intact tropical peat dome using field samplings and airborne LiDAR. *Ecological Applications*, *26*(2), 587–601. https://doi.org/10.1890/15-0017

Oksanen, J., Blanchet, F.G., Friendly, M., Kindt, R., Legendre, P., McGlinn, D., Minchin, P.R., O'Hara, R.B., Simpson, G.L., Solymos, P., Stevens, M.H., Szoecs, E., Wagner, H. (2019). Community ecology package. R package version 2.5.5.

Parker, G.G., Harding, D.J., Berger, M.L. (2004). A portable lidar system for rapid determination of forest canopy structure. *Journal of Applied Ecology*, *41*(4), 755–767. https://doi.org/10.1111/j.0021-8901.2004.00925.x

Parker, G.G., Harmon, M.E., Lefsky, M.A., Chen, J., Van Pelt, R., Weis, S.B., Thomas, S.C., Winner, W.E., Shaw, D.C., Frankling, J.F. (2004). Three-dimensional structure of an old-growth Pseudotsuga-Tsuga canopy and its implications for radiation balance, microclimate, and gas exchange. *Ecosystems*, *7*(5), 440-453. https://doi.org/10.1007/s10021-004-0136-5

R Development Core Team (2019). R: A language and environment for statistical computing. R Foundation for Statistical Computing, Vienna, Austria, ISBN 3-900051-07-0. http://www.R-project.org.

Roussel, J.R., Auty, D. (2018). LidR: Airborne LiDAR data manipulation and visualization for forestry applications. R package version 1.6.1.

Silva, C.A., Crookston, N.L., Hudak, A.T., Vierling L.A., Klauberg, C., Cardil, A. (2017). rLiDAR: LiDAR data processing and visualization. R package version 0.1.1.

Wallace, L., Lucieer, A., Malenovský, Z., Turner, D., Vopenka, P. (2016). Assessment of forest structure using two UAV techniques: A comparison of airborne laser scanning and Structure from Motion (SfM) point clouds. *Forests 7*(3), 62. https://doi.org/10.3390/f7030062

Yang, X., Schaaf, C., Strahler, A., Li, Z., Wang, Z., Yao, T., … Lovell, J. (2013). Studying canopy structure through 3-D reconstruction of point clouds from full-waveform terrestrial lidar. *IEEE International Geoscience and Remote Sensing Symposium 2013*, 3375–3378. https://doi.org/10.1109/IGARSS.2013.6723552

Zimble, D.A., Evans, D.L., Carlson, G.C., Parker, R.C., Grado, S.C., Gerard, P.D. (2003). Characterizing vertical forest structure using small-footprint airborne LiDAR. *Remote Sensing of Environment*, *87*(2–3), 171–182. https://doi.org/10.1016/S0034-4257(03)00139-1